A new species of the Ordovician horseshoe crab *Lunataspis*

James C. Lamsdell[1] , Phillip A. Isotalo[2], David M. Rudkin[3] and Markus J. Martin[4]

[1]Department of Geology and Geography, West Virginia University, 98 Beechurst Avenue, Morgantown, WV 26506, USA; [2]93 Napier Street, Kingston, Ontario K7L 4G2, Canada; [3]Department of Natural History, Royal Ontario Museum, 100 Queen's Park, Toronto, Ontario M5S 2C6, Canada and [4]371 Pawling St, Watertown, NY 13601, USA

CAMBRIDGE
UNIVERSITY PRESS

Abstract

Horseshoe crabs as a group are renowned for their morphological conservatism punctuated by marked shifts in morphology associated with the occupation of non-marine environments and have been suggested to exhibit a consistent developmental trajectory throughout their evolutionary history. Here, we report a new species of horseshoe crab from the Ordovician (Late Sandbian) of Kingston, Ontario, Canada, from juvenile and adult material. This new species provides critical insight into the ontogeny and morphology of the earliest horseshoe crabs, indicating that at least some Palaeozoic forms had freely articulating tergites anterior to the fused thoracetron and an opisthosoma comprising 13 segments.

1. Introduction

Xiphosurans (commonly referred to as horseshoe crabs) are aquatic chelicerate arthropods with an extensive fossil record stretching back to the Ordovician (Rudkin *et al.* 2008) but a seemingly low standing diversity with only 76 species described to date throughout the entirety of their 445 Ma evolutionary history (Lamsdell, 2020). Despite being rare components of aquatic ecosystems, the four extant horseshoe crab species have long been recognized as being biomedically important for vaccine production (Das *et al.* 2015) and keystone components of their ecosystems in need of active conservation (Karpanty *et al.* 2006), and are the focus of extensive research (Lamsdell, 2022*a*). Fossil horseshoe crabs have also been the subject of numerous evolutionary studies, mostly related to the notion that horseshoe crabs are quintessential 'living fossils' exhibiting low rates of evolutionary change manifesting in long-term bradytely and morphological stasis (Fisher, 1984, 1990; Kin & Błażejowski, 2014), potentially driven by a generalist ecology. This traditional narrative has been overturned in recent years, with extinct horseshoe crabs shown to have greater ecological and morphological diversity than modern forms (Lamsdell, 2016) and a number of xiphosuran clades exhibiting marked shifts in morphology linked to heterochronic shifts in development as they occupy non-marine environments (Lamsdell, 2021*a*, *b*). Despite these morphological and ecological changes, horseshoe crabs are thought to have maintained a consistent post-embryonic developmental trajectory (Lamsdell, 2021*a*; Bicknell *et al.* 2022) and exhibit a neuroanatomy conserved at least since the Carboniferous (Bicknell *et al.*, 2021*b*), making xiphosurans an important group for studying the patterns and drivers of mosaic evolution (Hopkins & Lidgard, 2012; Hunt *et al.* 2015).

Our understanding of horseshoe crab diversity trends has changed drastically in the last decade. The removal of synziphosurines – a polyphyletic grouping of stem and crown euchelicerates (Lamsdell, 2013; Lamsdell *et al.* 2015) – from Xiphosura reduced early Palaeozoic horseshoe crab diversity to a rump, while the synonymy of some 15 species of *Belinurus* (Lamsdell, 2022*b*) severely depleted the recognized acme of xiphosuran diversity during the Carboniferous. Conversely, the trough in diversity during the Jurassic has been somewhat ameliorated with the description of two new species from the Hettangian (Bicknell *et al.*, 2021*a*) and Sinemurian (Lamsdell *et al.* 2021). One trend that has remained consistent, however, is the paucity of horseshoe crab species early on in their evolutionary history, with only a single species currently described from the Ordovician (Rudkin *et al.* 2008) and none known from the Silurian. With the early evolution of the group so poorly represented in the fossil record, any new early Palaeozoic discoveries have the potential to provide critical information on horseshoe crab origins. Here, we describe three horseshoe crab specimens from the Upper Ordovician of Ontario, Canada, as a new species congeneric to *Lunataspis aurora*, the only other previously described Ordovician xiphosuran. Critically, this new species is represented by multiple instars and as such affords a view into xiphosuran ontogeny at the very start of their known fossil record, permitting exploration of whether the conserved xiphosuran developmental trajectory has been maintained since the origins of the clade.

2. Material and methods

2.a. Lunataspis *material and specimen visualization*

Lunataspis borealis sp. nov. is described from three specimens, all housed in the collections of the Royal Ontario Museum (ROM), Toronto, Canada, and recovered from Kingston, Ontario, Canada. The holotype specimen (ROM IP 64616) is a mostly complete adult individual while the two paratypes (ROM IP 64617 and 64618) are juveniles or subadults preserving the prosoma and thoracetron along with parts of the postabdomen. The fossil material was photographed using a Canon EOS 5D Mark IV digital camera with a Canon EF 100 mm Macro lens. All specimens were imaged immersed in ethanol under polarized light.

2.b. Geological setting

All specimens of *Lunataspis borealis* sp. nov. are derived from the Upper Member of the Gull River Formation, Simcoe Group, Upper Ordovician (Late Sandbian), where it is exposed in the north face of an inactive quarry on the east side of Division Street, south of Benson Street, Kingston, Ontario. Specimens were excavated from a shaly limestone interval *c.* 4 cm in thickness, immediately below a massive micritic unit in turn located 70–80 cm beneath the top of the exposed section. There is considerable historical controversy regarding the nomenclature of Upper Ordovician lithostratigraphic units in the Kingston area, with some authors having applied terminology based on that of correlative Black River Group strata in New York State (McFarlane, 1992; Cornell, 2000), while others employ the formational names established or modified by Liberty (1969, 1971) for the Lake Simcoe and Kingston areas in Ontario (Carson, 1982; LeBaron & Williams, 1990; Mitchell *et al.* 2004). Mapping by Carson (1982) shows the discovery quarry located in his middle member (3B) of a tripartite Gull River Formation. Subsequent revision (LeBaron & Williams, 1990) resulted in a local twofold division of the Gull River, with the discovery site falling within a redefined upper member. Following NYS terminology, McFarlane (1992) placed the uppermost portion of the discovery quarry section (approximately the top 6 m) in the Lowville Formation. Cornell (2000) showed what appears to be the same section high in the Lowville, equivalent to the upper Gull River Formation (Moore Hill beds of Okulitch (1939)). More recently, revised regional identification of key K-bentonite horizons and of biostratigraphically significant conodont faunas (Mitchell *et al.* 2004) suggests the discovery section falls in the M3 sequence of Holland and Patzkowsky (1996), correlative with the *Belodina compressa* Chronozone. We herein follow the scheme in use by the Ontario Geological Survey (Armstrong & Carter, 2010).

Late Ordovician strata in the Kingston area form part of a broad, warm-water carbonate shelf succession within the St Lawrence Platform tectonic province (Sanford, 1993). Deposition took place along the southern margin of equatorial Laurentia at *c.* 20° S latitude (Mac Niocaill *et al.* 1997). Near Kingston, gently southeastward-dipping Ordovician rocks are bounded to the north and east by the Frontenac Arch which brings underlying Proterozoic (Grenville Province) basement to the surface (Hewitt, 1964). The main expression of the arch lies less than 10 km from the discovery locality, but because the Precambrian surface has an irregular topographic relief, at several sites within 3–7 km of the quarry, granitic and metamorphic basement rocks come very close to the surface or are exposed as outliers. These Precambrian topographic highs represent small islands or shoal areas within the shallow Gull River sea, just offshore of the fully emergent arch. At some of these locations, so-called basal beds of the Shadow Lake Formation contain large angular fragments of Proterozoic crystalline rocks incorporated into high-energy beach sands, which is compelling evidence of an island shoreline probably within a few metres laterally. Gull River carbonates lie just above these basal beds. Fossil-bearing beds of the Upper Member of the Gull River Formation near the top of the discovery quarry were likely formed under oscillating but only slightly deeper (shallow subtidal/peritidal) and quieter water (lagoonal) conditions in a protected area amidst shoals and small islands. Bathyurine trilobite sclerites were found at the same shaly horizon and in direct association with one of the xiphosurid specimens. The thicker micritic beds above and below this horizon yielded a sparse normal marine fauna of isoteline and bathyurine trilobite sclerites, leperditiid valves, tetradiid fragments and strophomenate brachiopods.

It is unclear whether the xiphosuran fossils represent moults or carcasses. Trace fossils are present on the bedding surface immediately below the thin shaly interval in which the three specimens were found, but there is no obvious bioturbation within the shale itself. The available evidence suggests the specimens were buried rapidly in fine-grained sediment under relatively low-energy conditions, with minimal compaction and no subsequent physical or biological disturbance, resulting in unique preservation of the small, relatively intact, non-mineralized xiphosuran exoskeletons.

3. Systematic palaeontology

Chelicerata Heymons, 1901
Xiphosura Latreille, 1802
Xiphosurida Latreille, 1802
Lunataspis Rudkin, Young and Nowlan, 2008
Lunataspis borealis sp. nov.

Etymology. The species name *borealis* is Latin for 'northern' and refers to the northerly latitude from which the species is known.

Holotype. ROM IP 64616 (Fig. 1a, d), complete adult specimen in dorsal view preserving the dorsal prosomal carapace, thoracetron, postabdomen and telson.

Additional material. Paratypes ROM IP 64617 (Fig. 1b, e), incomplete juvenile or subadult specimen in dorsal view preserving dorsal prosomal carapace and thoracetron, and ROM IP 64618 (Fig. 1c, f), incomplete juvenile or subadult specimen in dorsal view preserving the dorsal prosomal carapace, thoracetron and postabdomen.

Localities and horizon. Upper Member of the Gull River Formation, Simcoe Group, Upper Ordovician (Late Sandbian), in Kingston, Ontario, Canada (44° 15′ 52.7″ N, 76° 29′ 46.3″ W).

Diagnosis. Lunataspis with cardiac node positioned at base of cardiac lobe; lateral eyes located along middle of prosomal carapace length.

Description. ROM IP 64616 comprises the prosomal carapace, thoracetron, postabdomen and telson in dorsal view preserved in positive relief. Maximum preserved length 37.0 mm, missing the very tip of the telson. Prosomal carapace 11.6 mm long, 18.8 mm wide, semicircular in outline. Cardiac lobe indistinct. Cardiac node, 1.0 mm long by 1.0 mm wide, located centrally at carapace posterior. Reniform lateral eyes faintly visible, 1.4 mm long by 0.5 mm wide, located 3.6 mm from carapace lateral margin and 5.6 mm from carapace posterior. Marginal rim indistinct. Genal spines extending 4.8 mm beyond prosomal carapace posterior, narrowing distally from width of 4.0 mm proximally. Thoracetron 7.7 mm long, 14.1 mm wide anteriorly narrowing
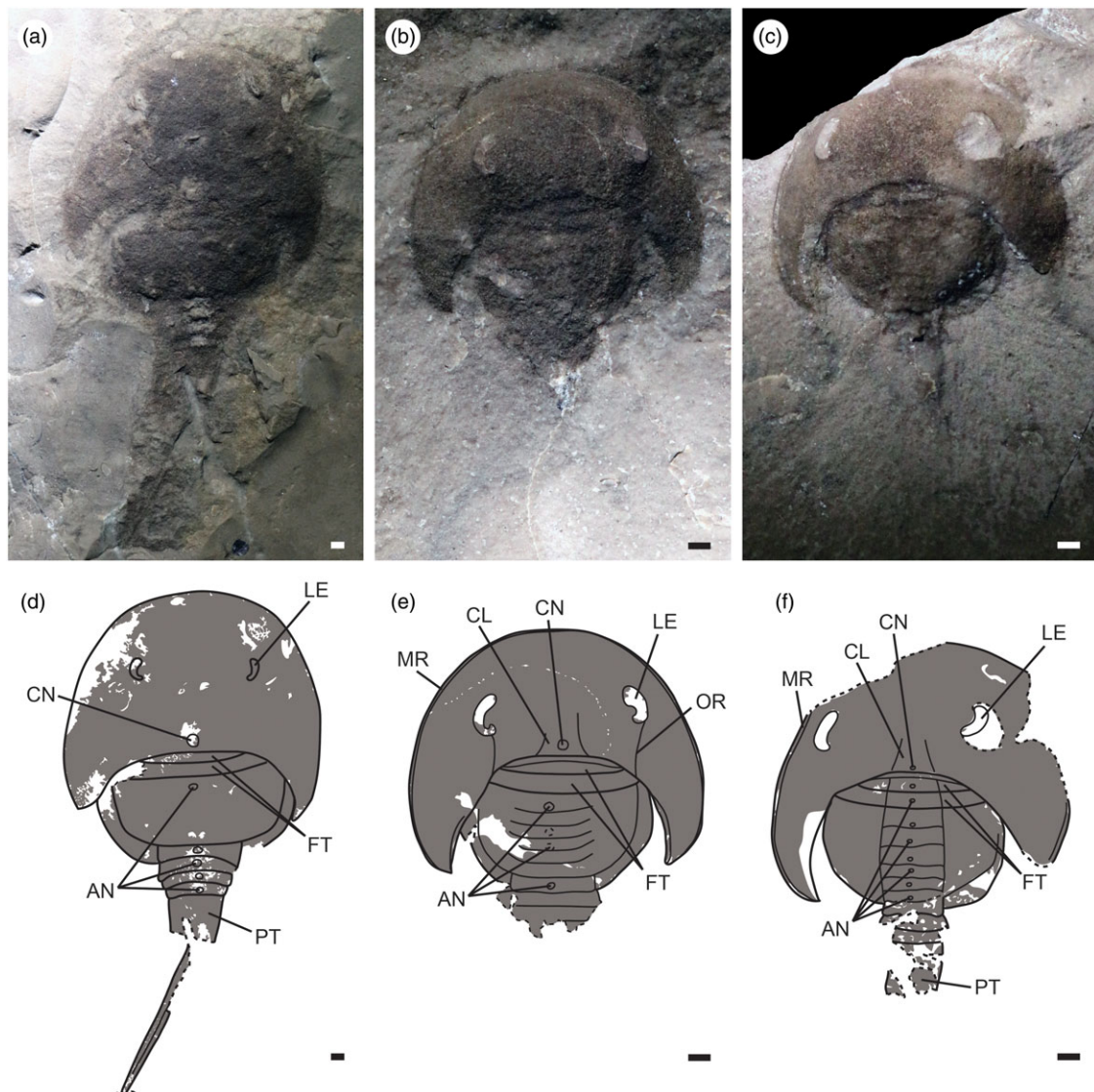
Fig. 1. (Colour online) *Lunataspis borealis* sp. nov. specimens and interpretive drawings. (a) ROM IP 64616. (b) ROM IP 64617. (c) ROM IP 64618. (d) Interpretive drawing of ROM IP 64616. (e) Interpretive drawing of ROM IP 64617. (f) ROM IP 64618. Grey indicates preservation of organic cuticular material. All scale bars = 1 mm. Abbreviations: AN, axial node; CL, cardiac lobe; CN, cardiac node; FT, free tergites; LE, lateral eye; MR, marginal rim; OR, ophthalmic ridge; PT, pretelson.

to 10.1 mm wide posteriorly, broadly rectangular in outline. Number of tergites in thoracetron unknown. First two thoracetron tergites freely articulating, first tergite 0.9 mm long, second tergite 1.0 mm long. Flattened pleural region, potentially corresponding to the ventral doublure, extends around the thoracetron margin posterior to the freely articulating segments and is 1.3 mm wide. Axial region of thoracetron indistinct. Vestigial differentiation of final thoracetron segment axis in line with thoracetron pleural region. Postabdomen composed of three freely articulating segments and pretelson. First postabdominal segment 1.0 mm long and 5.7 mm wide, second 0.9 mm long and 4.9 mm wide, third 0.8 mm long and 4.0 mm wide. Pretelson elongated, 3.2 mm long and 3.4 mm wide. Axial nodes, 0.8 mm long and 0.8 mm wide, present at thoracetron anterior and each postabdominal segment. Telson long, styliform, preserved length 12.5 mm, 0.9 mm wide.

ROM IP 64617 comprises the prosomal carapace, thoracetron, and proximal postabdominal segments in dorsal view preserved in negative relief. Maximum preserved length 13.7 mm, missing the

posterior postabdominal segments and telson. Prosomal carapace 5.8 mm long, 13.1 mm wide, lunate in outline. Cardiac lobe 2.0 mm wide at base. Cardiac node, 0.4 mm long by 0.4 mm wide, located centrally on cardiac lobe. Reniform lateral eyes, 1.7 mm long by 0.5 mm wide, located 2.2 mm from carapace lateral margin and 1.9 mm from carapace posterior. Faint ophthalmic ridge located posterior to lateral eyes, extending to carapace posterior in line with fulcrum of thoracetron pleural region. Narrow (0.2 mm) marginal rim extends to distal portion of genal spines. Genal spines extending 4.4 mm beyond prosomal carapace posterior, narrowing distally from width of 3.4 mm proximally. Thoracetron 5.9 mm long, 7.7 mm wide anteriorly narrowing to 5.3 mm wide posteriorly, semicircular in outline. Thoracetron composed of eight tergites. First two thoracetron tergites freely articulating, both tergites 0.7 mm long. Flattened pleural region, potentially corresponding to the ventral doublure, extends around the thoracetron margin posterior to the freely articulating segments and is 0.5 mm wide. Axial region of thoracetron exhibiting faintly visible vestigial

differentiation of six fused tergites, sixth axial segment in line with thoracetron pleural region. Postabdomen composed of at least three freely articulating segments. Axial nodes poorly preserved but appear to be present on fused thoracetron segments.

ROM IP 64618 comprises the prosomal carapace, thoracetron and postabdomen in dorsal view preserved in positive relief. Maximum preserved length 13.5 mm, missing the telson. Prosomal carapace 6.2 mm long, 13.7 mm wide, lunate in outline. Cardiac lobe 2.8 mm wide at base. Cardiac node, 0.4 mm long by 0.4 mm wide, located centrally on cardiac lobe. Reniform lateral eyes, 1.8 mm long by 0.6 mm wide, located 4.0 mm from carapace lateral margin and 2.1 mm from carapace posterior. Narrow (0.3 mm) marginal rim extends to distal portion of genal spines. Genal spines extending 5.2 mm beyond prosomal carapace posterior, narrowing distally from width of 2.6 mm proximally. Thoracetron 6.2 mm long, 8.6 mm wide anteriorly narrowing to 6.3 mm wide posteriorly, semicircular in outline. Thoracetron composed of eight tergites. First two thoracetron tergites freely articulating, both tergites 0.7 mm long. Flattened pleural region, potentially corresponding to the ventral doublure, extends around the thoracetron margin posterior to the freely articulating segments and is 0.5 mm wide. Axial region of thoracetron with axis margins in line with cardiac lobe. Vestigial differentiation of six fused thoracetron tergites visible within axis, sixth axial segment in line with thoracetron pleural region. Postabdomen composed of three freely articulating segments and pretelson. First postabdominal segment 0.5 mm long, second 0.5 mm long, third 0.4 mm long, lateral margins indistinct. Pretelson elongated, 2.4 mm long. Axial nodes, 0.3 mm long and 0.3 mm wide, present on thoracetron segments.

4. Discussion

Lunataspis borealis sp. nov. exhibits a number of traits considered diagnostic of the genus *Lunataspis*, including the large, lunate prosomal carapace with a low cardiac lobe and a shallow U-shaped posterior embayment (Rudkin *et al.* 2008). The original diagnosis for *Lunataspis* indicates that the thoracetron is completely fused and composed of six or seven sclerites while the postabdomen consists of three tergites with a medially constricted telson. *Lunataspis borealis*, however, possesses two freely articulating tergites anterior to a thoracetron comprising six sclerites with a postabdomen of four tergites, the last of which is an elongated pretelson. These differences would be enough to place the new species in a new genus; however, large specimens of *Lunataspis aurora* show that two freely articulating segments exist anterior to the thoracetron (Young *et al.* 2012) while other specimens demonstrate that the 'constriction' of the telson of *Lunataspis aurora* in the original description is actually the articulation between a narrow telson and an elongated pretelson (Rudkin & Young, 2009), as in *Lunataspis borealis*. The new species described here, while congeneric with *Lunataspis aurora*, can be clearly differentiated based on its position of a large node located at the base of the shallow cardiac lobe and the position of the lateral eyes along the median third of the carapace length compared to the posterior third in *Lunataspis aurora*. The discovery of *Lunataspis borealis* demonstrates that multiple roughly coeval species of *Lunataspis* occupied the shallow seas of Laurentia during the Late Ordovician and extends the range of the genus from Manitoba into eastern Ontario.

The three available specimens of *Lunataspis borealis* comprise at least two distinct instars, with the larger holotype (ROM IP

64616; Fig. 1a) representing an adult or subadult, while the paratypes (Fig. 1b, c) are smaller juvenile individuals. Although the ontogenetic data for the new species is limited to two instars, a number of changes are apparent. The overall proportions of the animal change, with the prosoma increasing from being equal in size to the thoracetron in juveniles to half again the thoracetron size in adults. Within the prosoma, the lateral eyes exhibit negative allometry, being proportionally smaller in the adult specimen compared to the juveniles, and shift to being more centrally positioned along the carapace length compared to their more posterior position in the juveniles. The genal spines also proportionally reduce in length, accounting for around a third of the total prosomal carapace length in the adult compared to just under half the prosomal carapace length in the juvenile specimens. The thoracetron also undergoes a shift from a semicircular outline in the juveniles to a markedly rectangular shape in the adult specimen.

The ontogeny of *Lunataspis borealis* reveals conflicting adherence to the generalized ontogenetic trajectories identified across Xiphosura (Lamsdell, 2021a), with different tagma (Lamsdell, 2013) exhibiting different trends, suggesting some degree of developmental modularity. The changes observed within the thoracetron, specifically the transition from a semicircular to a more angular outline and the apparent reduction of visible tergite margins and axial nodes, fit the previously identified trends. Conversely, the migration of the lateral eyes anteriorly as the organism matures, the decrease in the proportional length of the genal spines, and the negative allometry of the lateral eyes result in the structures of the prosoma exhibiting a general opposite trend to that inferred for other xiphosurans. Interestingly, a decrease in both the length of genal carapace extensions and lateral eye size is observed in eurypterid ontogeny (Lamsdell & Selden, 2013). As the generalized developmental trajectory for Xiphosura is recognized in both Belinurina and Limulina (Lamsdell, 2021a; Bicknell *et al.* 2022) it is possible that *Lunataspis*, which resolves as the basalmost xiphosuran outside of the Belinurina and Limulina clades, is exhibiting a mixture of ancestral and derived ontogenetic trajectories and that the highly conserved developmental trajectory of Xiphosura developed somewhere within its stem lineage.

Conflict of interest. None.

References

Armstrong DK and Carter TR (2010) The subsurface Paleozoic stratigraphy of Southern Ontario. *Ontario Geological Survey, Special Volume* **7**, 1–301.

Bicknell RDC, Hecker A and Heyng AM (2021a) New horseshoe crab fossil from Germany demonstrates post-Triassic extinction of Austrolimulidae. *Geological Magazine* **158**, 1461–71.

Bicknell RDC, Kimmig J, Budd GE, Legg DA, Bader KS, Haug C, Kaiser D, Laibl L, Tashman JN and Campione NE (2022) Habitat and developmental constraints drove 330 million years of horseshoe crab evolution. *Biological Journal of the Linnean Society* **136**, 155–72.

Bicknell RDC, Ortega-Hernández J, Edgecombe GD, Gaines RR and Paterson JR (2021b) Central nervous system of a 310-m.y.-old horseshoe crab: expanding the taphonomic window for nervous system preservation. *Geology* **49**, 1381–5.

Carson DM (1982) Paleozoic geology of the Gananoque-Wolfe Island area, southern Ontario. *Ontario Geological Survey Map* P. 2496.

Cornell SR (2000) *Sequence stratigraphy and event correlations of upper Black River and lower Trenton Group carbonates of northern New York State and southern Ontario, Canada.* MSc thesis, University of Cincinnati, Cincinnati, Ohio, USA. Published thesis.

Das AP, Bal B and Mahapatra PS (2015) Horseshoe crabs in modern day biotechnological applications. In *Changing Global Perspectives in Horseshoe Crab Biology, Conservation and Management* (eds RH Carmichael, ML Botton, PKS Shin and SG Cheung), pp. 463–74. New York: Springer.

Fisher DC (1984) The Xiphosurida: archetypes of bradytely? In *Living Fossils* (eds N Eldredge and SM Stanley), pp. 196–213. New York: Springer-Verlag.

Fisher DC (1990) Rates of evolution – living fossils. In *Palaeobiology* (eds DEG Briggs and PR Crowther), pp. 152–9. London: Blackwell Scientific.

Hewitt DF (1964) Geological notes for map numbers 2053 and 2054, Madoc – Gananoque Area. *Ontario Division of Mines, Geological Circular* 12, 1–33.

Heymons R (1901) Die Entwicklungsgeschichte der Scolopender. *Zoologica* 13, 1–244.

Holland SM and Patzkowsky ME (1996) Sequence stratigraphy and long-term paleoceanographic changes in the Middle and Upper Ordovician of eastern United States. In *Paleozoic Sequence Stratigraphy: Views from the North American Craton* (eds BJ Witzke, GA Ludvigson and J Day), pp. 117–29. Boulder, Colorado: Geological Society of America.

Hopkins MJ and Lidgard S (2012) Evolutionary mode routinely varies among morphological traits within fossil species. *Proceedings of the National Academy of Sciences of the United States of America* 109, 20520–5.

Hunt G, Hopkins MJ and Lidgard S (2015) Simple versus complex models of trait evolution and stasis as a response to environmental change. *Proceedings of the National Academy of Sciences of the United States of America* 112, 4885–90.

Karpanty SM, Fraser JD, Berkson J, Niles LJ, Dey A and Smith EP (2006) Horseshoe crab eggs determine red knot distribution in Delaware Bar. *Journal of Wildlife Management* 70, 1704–10.

Kin A and Błażejowski B (2014) The horseshoe crab of the genus *Limulus*: living fossil or stabilomorph? *PLOS ONE* 9, e108036. doi: 10.1371/journal.pone.0108036.

Lamsdell JC (2013) Revised systematics of Palaeozoic 'horseshoe crabs' and the myth of monophyletic Xiphosura. *Zoological Journal of the Linnean Society* 167, 1–27.

Lamsdell JC (2016) Horseshoe crab phylogeny and independent colonisations of freshwater: ecological invasion as a driver for morphological innovation. *Palaeontology* 59, 181–94.

Lamsdell JC (2020) The phylogeny and systematics of Xiphosura. *PeerJ* 8, e10431. doi: 10.7717/peerj.10431.

Lamsdell JC (2021a) A new method for quantifying heterochrony in evolutionary lineages. *Paleobiology* 47, 363–84.

Lamsdell JC (2021b) The conquest of spaces: exploring drivers of morphological shifts through phylogenetic palaeoecology. *Palaeogeography, Palaeoclimatology, Palaeoecology* 583, 110672. doi: 10.1016/j.palaeo.2021.110672.

Lamsdell JC (2022a) Evolutionary history of the dynamic horseshoe crab. *International Wader Studies* 21. doi: 10.18194/DB.00173.

Lamsdell JC (2022b) One name to rule them all: *Belinurus trilobitoides* (Buckland, 1837) is senior synonym to fourteen named species. *Journal of Paleontology* 96, 237–41.

Lamsdell JC, Briggs DEG, Liu HP, Witzke BJ and McKay RM (2015) A new Ordovician arthropod from the Winneshiek Lagerstätte of Iowa (USA) reveals the ground plan of eurypterids and chasmataspidids. *The Science of Nature* 102, 63. doi: 10.1007/s00114-015-1312-5.

Lamsdell JC and Selden PA (2013) Babes in the wood – a unique window into sea scorpion ontogeny. *BMC Evolutionary Biology* 13, 98. doi: 10.1186/1471-2148-13-98.

Lamsdell JC, Teruzzi G, Pasini G and Garassino A (2021) A new limulid (Chelicerata, Xiphosura) from the Lower Jurassic (Sinemurian) of Osteno, NW Italy. *Neues Jahrbuch für Geologie und Paläontologie – Abhandlungen* 300, 1–10. doi: 10.1127/njgpa/2021/0974.

Latreille PA (1802) *Histoire naturelle, générale et particulière, des Crustacés et des Insectes, vol. 3.* Paris: Dufart.

LeBaron PS and Williams DA (1990) Carbonate building stone resources of the Lake Simcoe – Kingston area, southeastern Ontario. *Ontario Geological Survey, Open File Report* 5730.

Liberty BA (1969) Paleozoic geology of the Lake Simcoe area, Ontario. *Geological Survey of Canada Memoirs* 355, 1–201.

Liberty BA (1971) Paleozoic geology of the Wolfe Island, Bath, Sydenham, and Gananoque map-areas. *Geological Survey of Canada Papers* 70-35, 1–12.

Mac Niocaill C, Van der Pluijm BA and Van der Voo R (1997) Ordovician paleogeography and the evolution of the Iapetus ocean. *Geology* 25, 159–62.

McFarlane RB (1992) *Stratigraphy, paleoenvironmental interpretation, and sequences of the Middle Ordovician Black River Group, Kingston, Ontario, Canada.* MSc thesis, Queen's University, Ontario, Canada. Published thesis.

Mitchell CE, Adhya S, Bergström SM, Joy MP and Delano JW (2004) Discovery of the Ordovician Millbrig K-bentonite Bed in the Trenton Group of New York State: implications for regional correlation and sequence stratigraphy in eastern North America. *Palaeogeography, Palaeoclimatology, Palaeoecology* 210, 331–46.

Okulitch VJ (1939) The Ordovician section at Coboconk, Ontario. *Transactions of the Canadian Institute* 22, 319–39.

Rudkin DM and Young GA (2009) Horseshoe crabs – an ancient ancestry revealed. In *Biology and Conservation of Horseshoe Crabs* (eds JT Tanacredi, ML Botton and D Smith), pp. 25–44. New York: Springer-Verlag.

Rudkin DM, Young GA and Nowlan GS (2008) The oldest horseshoe crab: a new xiphosurid from Late Ordovician Konservat-Lagerstätten deposits, Manitoba, Canada. *Palaeontology* 51, 1–9.

Sanford B (1993) Stratigraphic and structural framework of Upper Middle Ordovician rocks in the Head Lake-Burleigh Falls area of south-central Ontario. *Géographie Physique et Quaternaire* 47, 253–68.

Young GA, Rudkin DM, Dobrzanski EP, Robson SP, Cuggy MB, Demski MW and Thompson DP (2012) Great Canadian *Lagerstätten* 3. Late Ordovician Konservat-Lagerstätten in Manitoba. *Geoscience Canada* 39, 201–13.